Compositional dependence of the bowing parameter for highly strained InGaAs/GaAs quantum wells

T. K. Sharma,[1,*] R. Jangir,[1] S. Porwal,[1] R. Kumar,[1] Tapas Ganguli,[1]
M. Zorn,[2,†] U. Zeimer,[2] F. Bugge,[2] M. Weyers,[2] and S. M. Oak[1]
[1]*Semiconductor Laser Section, Raja Ramanna Centre for Advanced Technology, Indore 452 013, Madhya Pradesh, India*
[2]*Ferdinand-Braun-Institut fuer Hoechstfrequenztechnik, Gustav-Kirchhoff-Str. 4, 12489 Berlin, Germany*
(Received 4 May 2009; published 6 October 2009)

Highly strained InGaAs/GaAs quantum wells (QWs) are studied using the complementary spectroscopic and high-resolution x-ray diffraction (HRXRD) techniques. It is found that the QW features can be precisely identified by solving the Schrödinger equation for a rectangular shape QW, thus ignoring any indium segregation effect and considering only the compositional dependence of bowing parameter (C) while using the QW parameters obtained from HRXRD measurements. The compositional dependence of "C" for $In_xGa_{1-x}As$ QWs ($0.294 \leq x \leq 0.42$) can be given by a linear relationship of $C=0.3525+0.9028x$, which provides a conduction band offset (ΔE_c) of the functional form: $\Delta E_c=0.7529x+0.2917x^2-0.4785x^3$ using the band offset (Q_c) value of 0.53. It is also observed that Q_c is independent of the composition of QWs. Though the QW sample with the maximum strain showed some relaxation ($R \approx 3.4\%$) as measured by the reciprocal space mapping in HRXRD, still it is largely insignificant and does not affect the measured value of "C" for the present set of QW samples.

DOI: 10.1103/PhysRevB.80.165403 PACS number(s): 78.66.Fd, 68.65.Fg

I. INTRODUCTION

Highly strained $In_xGa_{1-x}As/GaAs$ quantum wells (QWs) are widely used for the development of laser diodes operating beyond 1.2 μm, which are a key components in the local area network (LAN) and metropolitan area network (MAN) links especially for the fiber-to-the-home applications.[1–4] Recently, such lasers with significantly improved device characteristics have been reported by several groups.[5–9] For MAN and LAN links, it is necessary to develop a QW laser operating at wavelengths longer than 1.2 μm.[3,10] For the long wavelength operation of InGaAs QW lasers, it is necessary that a sufficient amount of indium is incorporated into the QW. However, strain puts an upper limit on the indium content for a pseudomorphic InGaAs QW.[10,11] Earlier, we reported the metal organic vapor phase epitaxy (MOVPE) growth of highly strained InGaAs QWs with indium content exceeding 40% by using only the conventional sources.[10] Spectroscopic techniques play a vital role in the development of advanced semiconductor devices and in fact have been applied extensively to study strained InGaAs/GaAs QWs where an accurate knowledge of all QW transitions, as well as the barrier band gap energy is routinely obtained.[10–15] Modulation spectroscopic techniques in general have been extremely useful for studying moderately strained ($x \sim 0.2$) $In_xGa_{1-x}As/GaAs$ QW structures.[15–17] Complementary spectroscopic techniques such as photoluminescence (PL), photoreflectance (PR), and surface photovoltage spectroscopy (SPS), where in the PR and SPS technique one essentially measures the absorption spectrum of semiconductors are often applied to study such quantum structures.[11–18] Recently, we applied PL and SPS techniques to investigate InGaAs/GaAs QWs where it was demonstrated that SPS provides more information about QWs than the routinely used PL technique even at room temperature.[12] We were able to identify the QW transitions by numerically solving the Schrödinger equation using an envelope function approximation for a finite square potential well only for the lowest values of indium content ($x \sim 0.2$). We were unable to do a similar exercise for $In_xGa_{1-x}As$ ($x \geq 0.30$) QWs with large built-in strain where it was observed that even the ground state (GS) transition could not be matched accurately by using the QW parameters determined from high-resolution x-ray diffraction (HRXRD) measurements. Long back, a similar observation has been made by Muraki *et al.*[19] where they observed that one needs to choose a particular value of the band offset in order to match the GS energy measured by the PL experiments with the numerically calculated transitions energy. It was further observed by them that for a few InGaAs/GaAs QW samples which were grown at a higher temperature, an inclusion of the indium segregation effect was absolutely essential in order to get a genuine match between experiment and theory which was otherwise impossible simply by choosing an arbitrary value of the band offset.

In this paper, we present our results related to the spectroscopic investigation of highly strained InGaAs QWs where we obtained a reasonable match between experiment and theory with a perfect rectangular shape QW without any indium segregation. Unlike a constant value reported in the literature,[20] we found that the bowing parameter for $In_xGa_{1-x}As$ QWs ($0.294 \leq x \leq 0.42$) is rather compositional dependent. Our analysis is further supported by HRXRD measurements where we did not find any signature of indium segregation.

II. EXPERIMENTAL DETAILS

Highly strained $In_xGa_{1-x}As/GaAs$ QW samples were grown in a horizontal low-pressure MOVPE reactor (AIX 200/4) reactor with a rotating substrate holder on GaAs (001) substrates. Arsine (AsH_3) and the trimethyl compounds of gallium (TMGa) and indium (TMIn) were used as precursors. The indium content of QWs (x) was varied by changing

the TMIn supply in the gas phase x_v=p(TMIn)/[p(TMGa)+p(TMIn)] at a constant TMGa vapor pressure p(TMGa). The nominal thickness values for InGaAs QWs and GaAs barriers were 8 and 100 nm, respectively. In order to suppress the effect of indium segregation, the QW structures were grown at a lower temperature of ~500 °C. The details of MOVPE growth have been reported earlier.[10] HRXRD single scans (ω-2θ rocking curves) were performed by using a PANalytical X'Pert Pro MRD diffractometer, equipped with a Ge (2 2 0) monochromator (Bartels type, four reflections), with a beam divergence of ~12 arc-second in the scattering plane for Cu Kα1 x-rays (λ=1.5406 Å). All the HRXRD measurements were done with a 0.75° open detector parallel to the scattering plane.[6,11,21] The reciprocal lattice maps were measured using a hybrid monochromator (PANalytical model Hybrid 4x) at the input side and a Ge (2 2 0) two-crystal three-bounce monochromator before the detector.[22,23] The beam divergence achieved by the hybrid monochromator was ~18 arc-second. The acceptance angle for the three bounce Ge (2 2 0) monochromator before the detector was ~12 arc-second. QW parameters namely the thickness and composition (indium content) were measured from the HRXRD measurements by matching the measured diffraction pattern with simulated ones using the Takaji-Taupin equation implemented in the commercial software: X'pert epitaxy.[6,10,21–27]

All spectroscopic measurements were performed using conventional grating-based spectroscopy and lock-in amplifier techniques at room temperature (RT). PL[28] was excited with a diode laser operating at ~800 nm, dispersed with a 1/4 m monochromator and detected by using a Ge photodiode.[10] For PR measurements,[17,18,29,30] a 100 W quartz-tungsten-halogen (QTH) lamp along with a 1/4 m monochromator is used as the light source. The monochromator bandpass is kept lower than 4 nm. The light from the monochromator (probe beam) is focused onto the sample and the reflected beam is focused onto the detector. A chopped solid state laser (1 mw power) operating at 532 nm (pump beam) is used to modulate the built-in surface electric field. Using a lock-in amplifier at the chopping frequency (330 Hz) of the pump beam, one measures the change in reflectivity of the sample (ΔR) due to the modulation as a function of wavelength of the probe beam. The dc part of the signal from the detector, which is proportional to the reflectivity (R), is also extracted and the final spectrum $\Delta R/R$ is obtained by dividing the ac signal by the dc signal. For SPS measurements,[31,32] the same light source used in PR was used to measure essentially the absorption coefficient of QW samples.[11,12] A lock-in amplifier is used to measure the changes in surface potential induced by the resulting periodic generation and subsequent redistribution of excess carriers. The small AC voltage was measured in "soft contact" capacitor-like geometry, wherein a transparent conducting glass front electrode was pressed gently against the front surface of sample, whose back surface was attached with conducting silver paste to a flat grounded copper electrode. Other experimental details about SPS measurements have been published earlier.[33]

TABLE I. Layer structure details of five $In_xGa_{1-x}As/GaAs$ QW samples (A–E) obtained from the HRXRD measurement.

	QW parameters obtained from the HRXRD data		
Sample No.	Indium Content (x)	QW thickness (nm)	Cap layer thickness (nm)
Sample-A	0.294 ± 0.005	8.1 ± 0.1	78 ± 1
Sample-B	0.378 ± 0.005	7.8 ± 0.1	76 ± 1
Sample-C	0.395 ± 0.005	7.7 ± 0.1	76 ± 1
Sample-D	0.41 ± 0.005	7.8 ± 0.1	80 ± 1
Sample-E	0.42 ± 0.01	7.2 ± 0.2	72 ± 2

III. RESULTS AND DISCUSSION

Five QW samples (sample A–E) were studied during this work and the layer structure details obtained from the HRXRD measurements are shown in Table I. For HRXRD simulations, it was assumed that the QW layer is pseudomorphically strained i.e., no relaxation was considered. It is also of considerable interest to know about any possible layer relaxation in the highly strained QW samples since any such possibility might alter the measured values of the QW parameters in HRXRD experiments. Especially, in case of QW samples with large built-in strain (with indium content $\geq$0.40) some amount of relaxation (partial relaxation) is expected.[6,22–26] The issue of partial relaxation in highly strained InGaAs QWs and its impact on the measured values of QW parameters will be discussed in detail later.

Figure 1 shows an example of the complementary PL, PR, and SPS spectroscopic measurements performed on sample A at RT. Figure 1(a) shows the RT PL spectrum which was fitted with two Gaussian peaks representing two electronic transitions associated with the InGaAs/GaAs QW structure. The two transitions lie in close proximity of the two lowest energy features seen in the corresponding RT SPS graph, as shown schematically in Fig. 1(b) by the two vertical dotted lines at ~1.12 and 1.16 eV. There are other features seen in the SPS graph in Fig. 1(b), which are shown by the three vertical dotted lines on the higher energy side, at about 1.24, 1.28, and 1.36 eV, respectively. The signatures of the transitions seen in PL and SPS spectra are more clearly evident in the PR spectrum shown in Fig. 1(c), in form of sharp transitions seen almost at the same energy positions like in the PL and SPS spectra and marked by the five vertical dotted lines. The identification and origin of these features will be fully elucidated later. It is obvious from Fig. 1 that the QW features can be best examined using the PR technique. QW features seen in the PR spectrum are more in number when compared to the PL spectrum and sharper than those seen in the SPS spectrum. Thus PR is the most appropriate spectroscopic technique even for the investigation of highly strained InGaAs/GaAs QW structures. Therefore, for the rest of article, we focus mainly on the spectroscopic data obtained through PR measurements on the five QW samples whose layer details are shown in Table I. The PR spectrum can be represented theoretically by the well-known Aspnes function, given by[34]

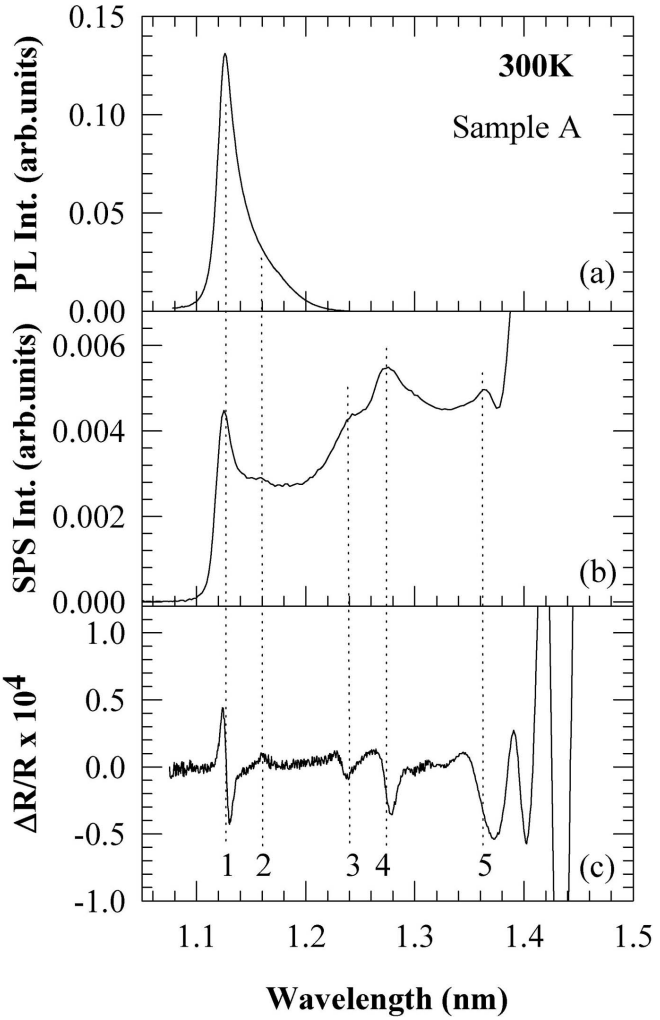

FIG. 1. RT (a) PL, (b) SPS, and (c) PR spectra of sample A. The vertical dotted lines correlate the individual components seen in three spectra.

$$\frac{\Delta R}{R} = \sum_{j=1}^{n} \mathrm{Re}\left\{A_j e^{i\theta_j}/(E - E_{0j} + i\Gamma_j)^{m_j}\right\}, \qquad (1)$$

where A_j is an amplitude, θ_j a phase angle, E_{0j} the critical point energy, Γ_j a broadening parameter and m_j an exponent which depends on the nature of the j^{th} critical point transition, and n is the number of critical point transitions. For example, for m=2, Eq. (1) corresponds to the first derivative of a Lorentzian peak, which is often used to fit the experimental PR spectra of excitonic transitions.[35] Fig. 2 shows the outcome of such a fitting exercise for sample A in the limited energy range of the spectrum shown earlier in Fig. 1(c) mainly covering sharp QW features (transitions "1"-to-"4" in Fig. 1). It is clearly seen from Fig. 2 that the QW PR spectrum can be fitted nicely with four sharp features having the functional form of Eq. (1) which therefore provide an accurate measurement of the energy position of QW transitions. The energy values of four QW transitions obtained after fitting with Eq. (1) are shown in Table II along with the results obtained from PL and SPS measurements.

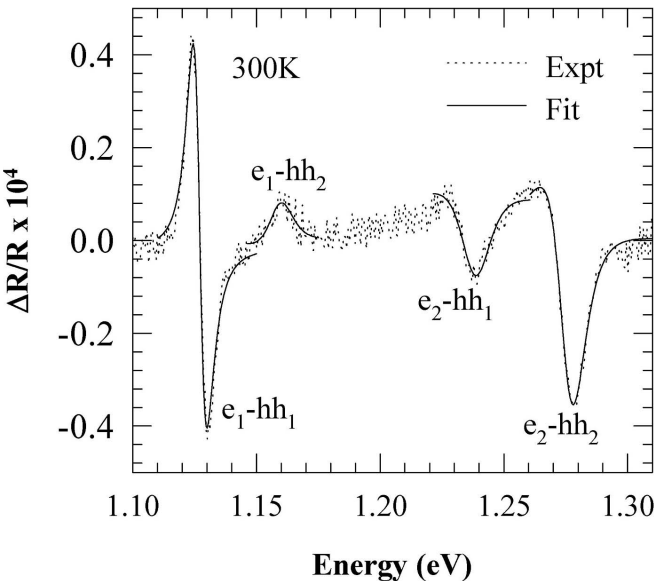

FIG. 2. Detail of the RT PR spectrum (dotted curve) of sample A over the energy region of the confined QW transitions, together with a fit by four features (full curves) using Aspnes function.

After the accurate determination of the energy of four QW features, the next obvious step is to identify the observed transitions. For this purpose, we calculated the energy of interband electronic transitions for the InGaAs QW by numerically solving the Schrödinger equation for a finite square potential well using the envelope function approximation.[11–13,16,17,19] The finite difference method (FDM) with a grid size of 1 Å was used to solve the Schrödinger equation where it is possible to work on symmetric/asymmetric (linearly graded at the upper interface) shape of the potential well.[36,37] The effect of strain in modifying the band structure at the Γ point was also taken into account, including the effect of spin-orbit coupling on the light-hole energy using the six-band k.p approach.[37,38] The material parameters were taken from literature.[20] The band offset ratio (Q_c) for the InGaAs/GaAs QW was taken initially as 58%[13] (Q_c is defined as $\Delta E_c/\Delta E_g$, with ΔE_c as the conduction band offset and ΔE_g being the difference between the GaAs barrier and the strained InGaAs well material heavy-hole band gaps). The thickness and composition of the QW for these calculations were taken from the HRXRD measurements, which are summarized in Table I. Following the numerical approach mentioned above, we calculated the energies of the interband QW transitions with a few possible sets of QW parameters for sample A and the simulation results are summarized in Table III. It was found that the calculated energy of the GS QW transition i.e., e_1-hh_1 (H11 for short) by using the QW parameters of sample A from Table I was larger by 27 meV when compared with the measured value shown in Table II. As mentioned earlier, a similar observation was made by Muraki *et al.*[19] for the same QW system where they were able to get a reasonable match between theory and experiment by carefully choosing an appropriate value of the band offset. The issue of a correct value of Q_c for this material system has been a matter of controversy[39] and people have reported values ranging from

TABLE II. Summary of all the spectroscopy data analysis for sample A. Error bars in the fitted values are much smaller than the energy changes produced by the error bars in QW parameters shown in Table I.

	Energy of Interband electronic transitions			
Experiment	Transition "1" (eV)	Transition "2" (eV)	Transition "3" (eV)	Transition "4" (eV)
PL	1.125	1.150	-NA-	-NA-
PR	1.127	1.159	1.238	1.276
SPS	1.123	1.160	1.240	1.276

0.4 to 0.8[40] for QW samples grown under different conditions. It has been measured by several techniques like capacitance voltage profiling,[39–42] deep level transient spectroscopy,[41,43] and spectroscopic techniques including modulation spectroscopy.[14,16,17,19,27,40,44–55] It has been even shown to vary with the composition of $In_xGa_{1-x}As/GaAs$ QWs.[17,40,46] Hence, by noting the fact that Q_c depends upon several factors, we tried to choose an appropriate value of Q_c with the hope that it will provide the expected energy values of QW transitions matching with the experimental results summarized in Table II. However, to our surprise, such an exercise proved fruitless since even the GS energy could not be matched by simply varying the value of Q_c. Under such circumstances, Muraki *et al.*[19] pointed out the importance of indium segregation for InGaAs/GaAs QW samples where they could get a reasonable match for the GS feature by assuming an asymmetric shape of the QW. Although, they said that the effect of indium segregation is not important for the MOVPE growth (the technique used here) yet we tried to consider the effect of indium segregation in two ways i.e., (i) by solving the Schrödinger equation using finite difference method for an asymmetric shape of the QW[13] (caused by probable indium segregation near the upper interface like Muraki *et al.*[19]), and (ii) by assuming that the $In_xGa_{1-x}As$ QW as a whole has either a larger thickness or higher indium content when compared with the measured values obtained from the HRXRD technique, respectively. We calculated the energy of QW transitions by varying either the QW thickness (where GS could be matched for 135 Å) or indium content (where GS could be matched for 0.324, also a more complicated asymmetrical profile assuming indium segregation) in order to match the measured values shown in Table II. We also tried to vary both the QW parameters following Hosea *et al.*[16] However, all these attempts were again largely unsuccessful since although an excellent match between theory and experiment could be achieved for the GS in each case but no satisfactory agreement was possible for the other sharp features shown in Fig. 2.

The importance of such a desired agreement between theory and experiment for the high energy QW transitions (in addition to the GS) has been suggested long back by Muraki *et al.*[19] Along with the increased value of the indium content (0.324 against the measured value of 0.294 from HRXRD), we also tried to vary Q_c for $In_xGa_{1-x}As$ QW as shown in Fig. 3 where we plot the calculated values of five QW transitions i.e., H11, H12, H21, H22 and e_1-lh_1 (L11 for short) with Q_c. For these calculations, the QW thickness was taken from Table I (sample A). The horizontal lines in this graph indicate the measured values of four transitions ("1"-to-"4") from Fig. 2. Surprisingly, a satisfactory match between theory and experiment could be obtained for a Q_c value of ~0.52 as shown in Fig. 3 and also summarized in Table III. On the other hand, when a similar exercise was done with variation of Q_c by keeping the indium-content constant (0.294) and choosing a large QW thickness of 135 Å, no such agreement could be obtained for the high energy features. Similar efforts by using an asymmetric shape of the QW for considering the effect of indium segregation were also unsuccessful as can be seen from the last row in Table III. Hence, it seems plausible that the QW composition measured by HRXRD is

TABLE III. Numerical simulation results for an InGaAs/GaAs QW (sample A) with several combinations of the layer parameters. The values shown in bold letters are the best match when compared with PR results summarized in Table II. The last row shows the best match when indium segregation is taken into account.

				Calculated energy of various interband electronic transitions (eV)			
Simulations	Indium Content	Thickness (Å)	Bowing parameter	H11	H12	H21	H22
With rectangular shape QW	0.294	81	0.477	1.154	1.185	1.161	1.292
	0.324	**81**	**0.477**	**1.127**	**1.159**	**1.240**	**1.273**
	0.294	135	0.477	1.127	1.140	1.188	1.201
	0.324	73.5	0.477	1.135	1.172	1.256	1.293
	0.294	**81**	**0.619**	**1.127**	**1.158**	**1.240**	**1.272**
With indium segregation	0.364, 0.31-to-0.16	40, 50 graded	0.477	1.127	1.178	1.236	1.285

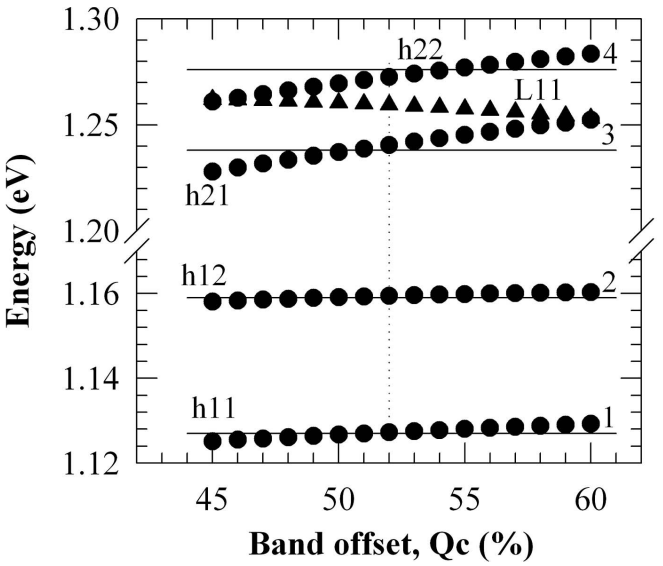

FIG. 3. Variation of the calculated energies of five QW transitions as a function of band offset (Q_c), for a 81 Å thick $In_{0.324}Ga_{0.676}As$ QW with GaAs barriers. The horizontal lines show the fitted energy values for the four QW features from the fit in Fig. 2. The vertical dotted line shows the possible Q_c value needed to match the various calculated transition energies to the fitted values. The light hole related transition (L11) does not find any reasonable match here.

possibly inaccurate. However, the discrepancy of about 3% (0.324 against 0.294, as seen from the first two rows of Table III) in HRXRD looks significantly high and it is highly desirable to know about the maximum amount of error in HRXRD measurements. Figure 4(a) shows the measured and simulated diffraction pattern for sample A, where the simulated pattern has been vertically shifted downward for the clarity in viewing. A clear observation of Pendellösung fringes around the GaAs substrate peak indicates a good crystalline quality of the sample[9,12] and provides an accurate measurement of composition and thickness of the QW as shown in Table I. In Fig. 4(b), we present the simulated patterns for an increased indium content of 32.4% while keeping the same QW thickness (as desired by the aforementioned quantum mechanical numerical simulations). It is obvious that this simulated pattern is entirely different than the one needed to match the experimental HRXRD pattern. Similarly, the simulated pattern of a QW with increased thickness i.e., 135 Å (against the measure value of 81 Å) is also significantly different. It is well known that the HRXRD measurements for strained InGaAs/GaAs QW are actually sensitive to the product of thickness and strain of QW[13] (not the individual entity) and hence, it is possible that the strained QW might have some small domains of high indium content (32.4% indium) but with reduced QW thickness (73.5 Å, in order to keep the product constant). It is clear from Fig. 4(c) that the HRXRD measurements rules out any such possibility. Moreover, as shown in Table III, such a combination of QW parameters does not even provide the correct GS information.

Finally, as shown in the last row of Table III, it is possible to get an approximate match for the QW transitions for an

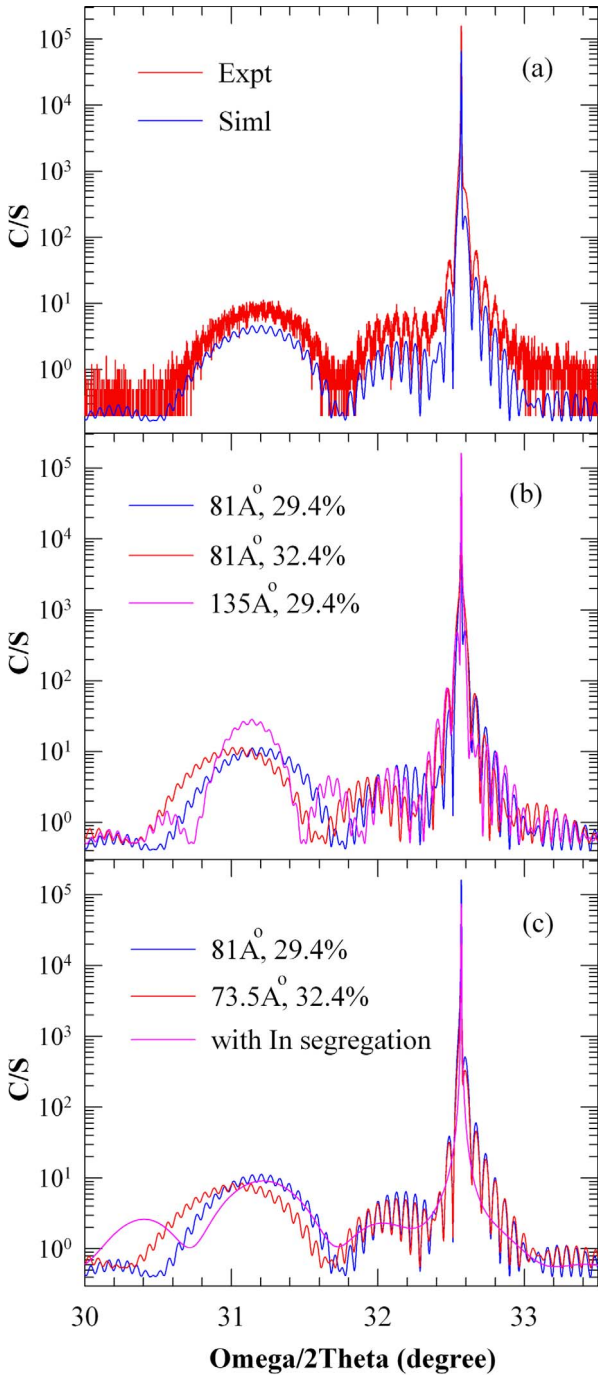

FIG. 4. (Color online) (a) HRXRD rocking curve for sample A along with the simulated one, note that the simulated pattern has been vertically shifted downward for clarity in viewing, (b) three simulated HRXRD patterns with different QW composition and width parameters, (c) two simulated HRXRD patterns where the product of strain and QW thickness was kept constant. Note that the Pendellösung fringes around the GaAs substrate feature are identical for the two patterns but the QW feature is entirely different. We also plot the simulation for a graded QW with indium segregation, which clearly discards any such possibility when compared with the experimental data shown in Fig. 4(a). Note that the second simulated pattern (32.4% In) has been vertically shifted downward for the clarity in viewing. Also note the matched simulated pattern (81 Å, 29%) is plotted in all the three graphs for comparison.

asymmetrically shaped QW by considering the effect of indium segregation.[19] It should be noted that the GS could be matched in several ways by varying the parameters of the asymmetric QW profile and the best combination obtained for all the QW transitions is only shown in Table III. However, HRXRD simulation again discards any such possibility. First, we do not anticipate such large variation in the QW composition as required by the asymmetric QW profile and second the HRXRD pattern simulated for such a profile significantly differs from the measured one as clearly shown in Fig. 4(c). It clearly shows that the effect of indium segregation has been largely suppressed by choosing a lower growth temperature of ~500 °C in MOVPE. We find its signature neither in spectroscopic nor HRXRD measurements. Hence, the measured values of QW parameters in HRXRD are highly genuine within the error bars shown in Table I.

In fact, similar to Sample A, we did the same analysis (by keeping the QW thickness constant while varying the indium content) for all the QW samples and could get a reasonable agreement between theory and experiment but the maximum discrepancy in QW composition was as high as 7%. Although, it is known that the errors in QW parameters (obtained from HRXRD measurements) increases with strain in the QW due to several reasons yet an inconsistency of ~7% is far beyond our error bars ($x \pm 1\%$, ± 2 Å for sample E) defined in our HRXRD results presented here. Hosea *et al.*[16] also made a similar observation earlier where they found that they need to increase the indium content by 1%–3% and the QW thickness by 1–6 Å in order to match even the GS energy. However, neither Muraki *et al.*,[19] nor Hosea *et al.*[16] presented any supporting high-quality HRXRD data to confirm their claims. It is obvious from Fig. 4(a) where an excellent agreement is clearly observed between the simulated and measured diffraction pattern and further from the HRXRD simulation seen in Figs. 4(b) and 4(c) that the source of anomaly for the QW parameters between the two measurements i.e., HRXRD and PR lies somewhere else. In fact, it was mainly this reason that motivated us to look for an alternate and more realistic source of inconsistency between the two measurements which subsequently resulted into the discovery of the compositional dependence of bowing parameter for highly strained InGaAs/GaAs QWs.

As mentioned above, under the circumstances when the agreement between theory and experiment is poor for QW transitions, we need to vary either the QW thickness or composition while keeping the other parameter constant. However, as obvious from the Tables II and III, a reasonable match was obtained only when we kept the QW size constant and increase the indium content. Since, this resulted in a large inconsistency between the QW parameters obtained from the two measurements, i.e., HRXRD and PR, an alternate way to achieve a satisfactory agreement between theory and experiment is desirable. Although an attempt of varying the QW composition in numerical calculations (irrespective of its prediction of correct energies for QW transitions) is highly unrealistic, nevertheless it provides a clear hint. It can be easily understood that by increasing the indium content of the QW, we in principle reduce the bulk band gap of the strained InGaAs material whereas the separation of energy levels within the QW remains largely unaffected. On the other hand, when we tried to vary the QW size while keeping the indium content constant, it did not provide the correct energy position of the excited state transitions as shown in Table III. This is due to the fact that a variation of QW thickness basically alters the separation of energy levels within the QW. Since, an increase of the indium content in InGaAs/GaAs QWs always moves the energy levels within the QW vertically downwards while maintaining their respective separation. We therefore need to look for an alternative method for varying the bulk band gap of strained InGaAs material in addition to its usual dependence on the indium content.

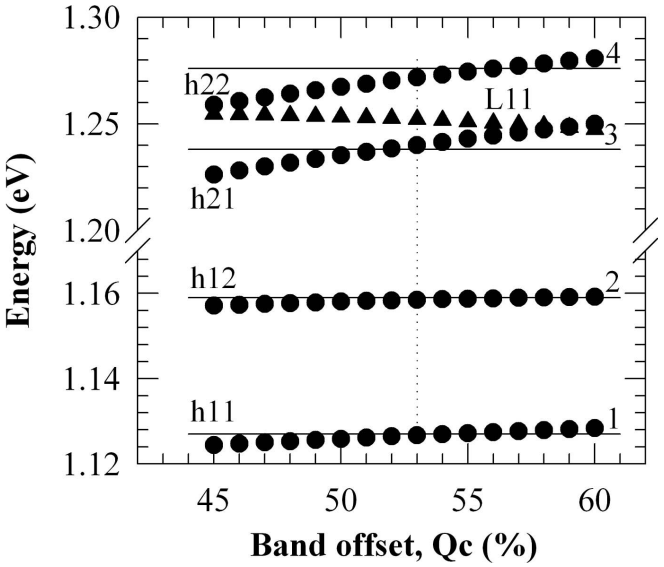

FIG. 5. Variation of the calculated energies of five QW transitions as a function of band offset (Q_c), for a 81 Å thick $In_{0.294}Ga_{0.706}As$ QW with GaAs barriers. The horizontal lines show the fitted energy values for the four QW features from the fit in Fig. 2. The vertical dotted line shows the possible Q_c value needed to match the various calculated transition energies to the fitted values. The light hole related transition (L11) does not find any reasonable match here.

We know from literature[20] that such an example already exists for $Al_xGa_{1-x}As$ where it has been shown that the bowing parameter for this particular alloy depends upon its composition. On the other hand, it is considered to be independent of composition for InGaAs where it is expected to have a constant value of 0.477.[20] However, our results described above suggest that this may not be true in case of highly strained InGaAs/GaAs QW structures. In our numerical simulations, we in fact then tried to choose an appropriate value of the bowing parameter (such that the desired strained heavy-hole band gap for the InGaAs QWs could be matched) while keeping the composition and thickness as obtained from the HRXRD measurements. An outcome of this exercise is shown in Fig. 5 where we plot the energy values of five QW transitions with Q_c where the bowing parameter was taken to be 0.619 instead of its usual value of 0.477. The solid lines in Fig. 5 show the positions of QW transitions obtained from the analysis of PR data shown in Fig. 2. It is obvious that a nice agreement between theory and experiment is obtained like shown earlier in Fig. 3. Hence, there is

no inconsistency as such between the two measurements i.e., PR and HRXRD. Features "1," "2," "3," and "4" could be therefore identified as H11, H12, H21, and H22 interband electronic transitions of the InGaAs QW. It could be confirmed even for the feature "5" in Fig. 1, which is expected to be e_2-hh_4 (H24 for short). In fact, the theory did not predict any confined state QW transitions above 1.4 eV and hence all the further features seen after H24 in Fig. 1 are related to the GaAs barrier. We do not observe any signature of a light holes related transition in our spectroscopic measurements as can be seen from Fig. 5. It should be noted that the effect of indium segregation is expected to be important even for the MOVPE growth process[56] and therefore similar to the MBE growth,[19,46] it is desired to grow the QW structures at relatively low temperatures in order to nullify the effect of unwanted indium segregation. Since the QW samples studied here were grown at relatively lower temperature (~500 °C),[10] we did not see any signature of indium segregation. HRXRD measurements also did not support any such behavior related to indium segregation in our samples as discussed earlier.

We then applied the same analytical procedure for all the five InGaAs/GaAs QW samples with their individual layer structure as shown in Table I. For the purpose of clarity, we present only the GS PR feature for these five samples in Fig. 6 along with its simulated counterpart using the Aspnes line shapes given by Eq. (1). A clean signature of GS QW feature in the PR spectrum of all the five samples is recorded. Although, the signal intensity drops with an increase in the built-in strain (indium content) possibly due to the poor crystalline and interfacial quality yet the features are in general clearer and sharper when compared with our SPS results presented earlier on the same set of samples.[12] A similar observation was made by us earlier[12] from the PL measurements on the same set of samples where the PL intensity was found to reduce when one approaches a critical value of the indium content for InGaAs QW. Fuji *et al.*[24] also made a similar observation earlier where they observed that the PL intensity decayed exponentially after a critical layer composition was reached. They described this behavior as a symptom of the lattice relaxation. However, we find that the critical layer composition in our case is found to be much larger and this may be simply related to the MOVPE growth at comparatively lower temperatures in our case.[10,12] A similar observation has also been made by Wei *et al.*[57] for QW samples grown by MBE at low temperatures. An information related to the lattice relaxation can be obtained from the HRXRD measurements where a degradation of the crystalline and interfacial quality is normally indicated by the disappearance of Pendellösung fringes for high values of indium content which is related to the fluctuations in the QW thickness and composition.[10,12] Such type of degradation is normally related to the partial relaxation of InGaAs QW layer.[6,23–26] More details about the relaxation of QW layer in our samples will be presented in the later part of this article.

It is obvious from Fig. 6 that the GS energy redshifts with the enhancement of indium content supporting our earlier observations from the PL and SPS measurements which is further summarized in Fig. 7. Similar to the reports available in literature,[55,58] we also find that the GS energy can be represented by a simple linear relation with indium content of the QW i.e., $E_o(eV)=1.446-1.091x$ for $In_xGa_{1-x}As$ QWs ($0.294 \leq x \leq 0.42$). Such a simple relationship for the emission energy (wavelength) of highly strained InGaAs/GaAs QW structures should be very useful for the material growers. It is also noticed that the broadening parameter "Γ" (described in Eq. (1)) initially shows a gradual increase with built-in strain (indium content) and then suddenly shows a significant change in the slope once a threshold value of strain is reached (for $x \sim 0.40$). It is therefore anticipated that the dominant scattering mechanisms are different in the two regions across the threshold composition ($x^{th} \sim 0.40$) of InGaAs QWs. Using the exciton-optical-phonon coupling model in which free excitons scatter off the longitudinal optical (LO) phonons, Shen *et al.*[51] suggested that the homogeneous part, i.e., Γ_h (which is a measure of the exciton-phonon coupling) is the dominant scattering mechanism at

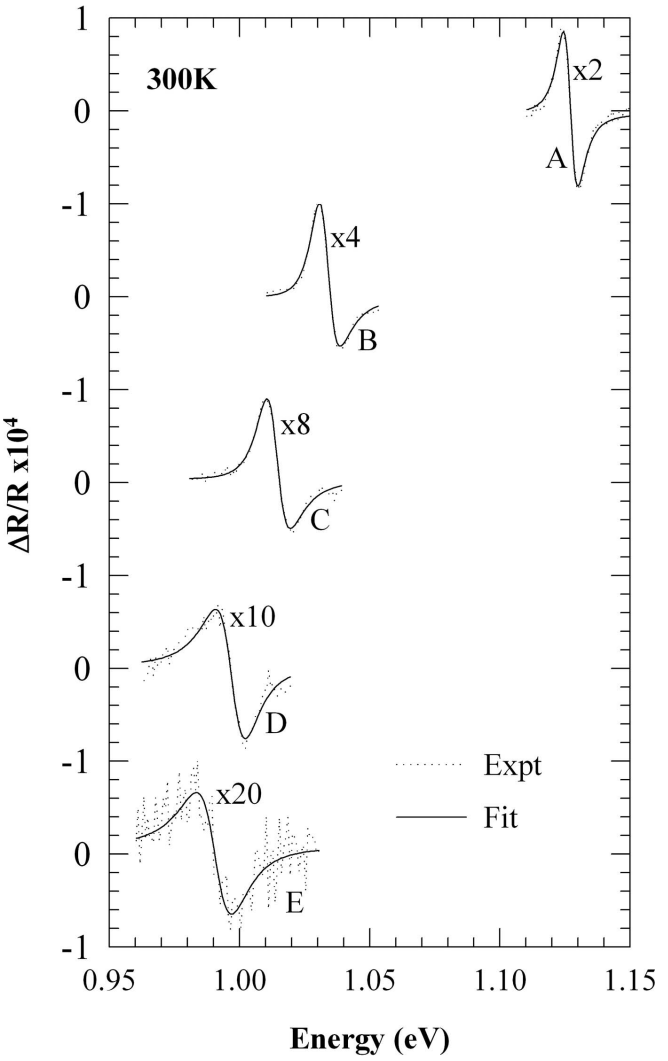

FIG. 6. RT PR spectra (dotted curves) showing only the ground state feature of the five $In_xGa_{1-x}As/GaAs$ QWs (samples A–E). The PR features has been magnified by the corresponding numbers for the purpose of clarity in viewing. Corresponding fitted spectra for the five QW samples using Aspnes line shape are also plotted in the same graph.

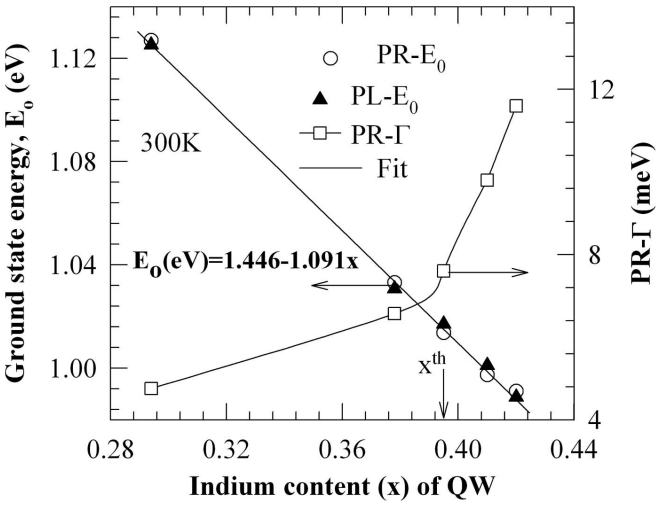

FIG. 7. A plot of the ground state energies (E_o) of five QW transitions determined from the PL and PR measurements as a function of indium content of InGaAs QWs (left axis), also shown is the fitted curve using a linear relationship with indium-content as shown in the graph. On the right axis, we plot the broadening parameter 'Γ' described in Aspnes line shape for the PR spectra with indium content, which show two distinct regions indicating a threshold indium content (x^{th}) beyond, which one sees a fast degradation in the crystalline and/or interfacial quality.

room temperature for strained InGaAs QWs. A sudden increase in the Γ values with indium content as shown in Fig. 7 indicates that the temperature independent inhomogeneous line width, i.e., Γ_i (which is a measure of the interface roughness and alloy disorder) becomes significant for the highly strained InGaAs QWs even at room temperature once the threshold composition is reached. In corroboration with the well established PL techqniue,[3,5–10] PR spectroscopy thus provides a very simple procedure for deciding the maximum indium content of highly strained InGaAs QWs for the development of long-wavelength laser diodes. It suggests that one needs to choose an optimum indium content below the threshold value (x^{th}) shown in Fig. 7 in order to anticipate a reasonable threshold current density of the laser diodes made using highly strained InGaAs QWs. Highly strained InGaAs QW lasers reported earlier[3,10] were fabricated using the QW samples B and C where the indium content really lies below the threshold value shown in Fig. 7.

After analysis of PR data for all QW samples, it is of interest to know the values of the bowing parameter needed to predict the upward transitions seen in PR spectra by utilizing the QW parameters measured from HRXRD. We could get a reasonable match between the theory and experiment for all five samples and the energy values of QW transitions both the experimental and simulated ones are presented in Table IV. Since, we could match several QW transitions except for sample E, where only GS was seen in the PR spectrum (due to the inferior sample quality/very high strain) by using the QW parameters determined by HRXRD, our analysis for the values of the bowing parameter is more realistic as suggested earlier by Muraki *et al.*[19] Fig. 8 shows a plot of the bowing parameter for $In_xGa_{1-x}As/GaAs$ QWs with built-in strain (indium content) where a linear behavior is obviously seen. The compositional dependence of bowing parameter for InGaAs QWs ($0.294 \leq x \leq 0.42$) is given by the following linear relationship i.e., $C=0.3525+0.9028x$. Zubkov *et al.*[42] reported a quadratic concentration dependence of the conduction band offset in case of medium strained InGaAs QWs ($0.06 \leq x \leq 0.29$) where the bowing parameter was expected to be independent of the QW composition. It is found here that the bowing parameter for highly strained InGaAs QWs shows a linear relationship with the indium-content (strain), which provides a conduction band offset of the functional form: $\Delta E_c=0.7529x+0.2917x^2-0.4785x^3$ using the band offset value of 0.53. It is also found here that the band offset is independent of the composition for $In_xGa_{1-x}As/GaAs$

TABLE IV. Summary of the spectroscopy data analysis along with the numerical simulation results for all the five InGaAs/GaAs QWs (samples A to E). Indium-content and the thickness of QWs were obtained from the HRXRD measurements whereas the bowing parameter values were calculated from the best match of PR data with the numerical simulations. The error bars in the fitted values are much smaller than the energy change produced by the error bar in QW composition shown in Table I.

					Energy of interband electronic transitions			
Sample No.	Experiment/ Simulations	Indium Content (x)	Thickness (Å)	Bowing parameter	Transition "1" (eV)	Transition "2" (eV)	Transition "3" (eV)	Transition "4" (eV)
Sample A	PR				1.127	1.159	1.238	1.276
	Simulation	0.294	81	0.619	1.127	1.158	1.240	1.272
Sample B	PR				1.033	1.066	1.166	1.207
	Simulation	0.378	78	0.691	1.033	1.068	1.170	1.206
Sample C	PR				1.014	1.049	1.154	1.314
	Simulation	0.395	77	0.706	1.014	1.050	1.157	1.327
Sample D	PR				0.997	1.024	1.141	-NA-
	Simulation	0.41	78	0.714	0.997	1.033	1.141	1.177
Sample E	PR				0.991	-NA-	-NA-	-NA-
	Simulation	0.42	72	0.736	0.991	1.032	1.149	1.338

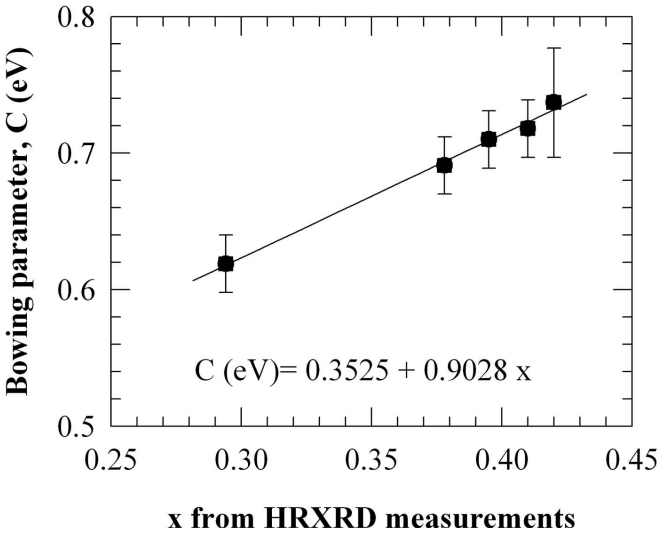

FIG. 8. A plot of the bowing parameter (c) with indium content for highly strained InGaAs/GaAs QWs. Error bars are mainly due to the errors in QW parameters determined from the HRXRD measurements with a relatively large error in case of sample E due to partial relaxation.

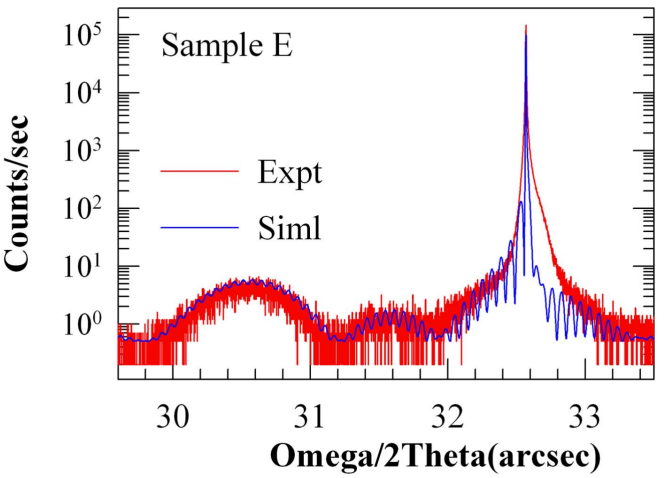

FIG. 9. (Color online) Experimental and simulated HRXRD rocking curves for sample E. Note the disappearance of the Pendellösung fringes in the experimental curve due to poor crystalline and interface quality because of very high built-in strain. Even the GaAs feature has been modified toward higher angles indicating tensile strain in the cap GaAs layer due to a partial relaxation of the InGaAs QW.

$(0.294 \leq x \leq 0.42)$ QWs. Finally, it is worthwhile to discuss the origin of the concentration dependence of bowing parameter in highly strained InGaAs QWs. The bowing parameter (C) is expected to have two components,[59] where the component "C_i" arises simply because of the dependence of the energy gap (E_g) on the lattice constant while the other component "C_e" is associated with disorder. Disorder produces potential fluctuations which in general scatter electrons and mix band states, derives states at the bottom (top) of the conduction (valence) band, respectively, and thus, reduces the band gap. From the HRXRD experiments and subsequent PR data analysis, it is clear that the disorder term "C_e" of the bowing parameters becomes important in case of highly strained InGaAs QW which makes the bowing parameter concentration dependent. The error bars in Fig. 8 arise due to the uncertainties in QW parameters obtained from HRXRD measurements (as shown in Table I) with a large error bar for sample E simply due to its poor crystalline and interfacial quality. A high accuracy in HRXRD simulations comes from the fine Pendellösung fringes (cap layer fringes) where the respective positions of peak and valleys are sensitive to the product of strain and QW thickness.[13] The HRXRD pattern for sample E is presented in Fig. 9 along with its simulated counterpart. Although, the QW feature is clearly visible at ~30.5° yet the disappearance of Pendellösung fringes increases the error in QW parameters which provides a large error bar in the bowing parameter value as indicated in Fig. 8.[60] Similar observations have been made earlier by Chen *et al.*[26] where they observed that the interference pattern in HRXRD pattern disappeared when $In_{0.2}Ga_{0.8}As$ QW layer exceeded 30 nm in thickness. They also observed a bump on the right shoulder of the GaAs peak like the one seen here in Fig. 9 suggesting that the top GaAs layer is being compressed in the growth direction by the partially relaxed InGaAs layer. A reliable information about the partially relaxation of InGaAs layer can be obtained from the reciprocal space mapping (two-axis scan) in HRXRD experiments for an asymmetric e.g., (224) reflection.[23,25,26]

Figure 10 shows two such asymmetrical reciprocal space maps for two samples (A and E), respectively, where it can be seen easily that the QW layer in sample A [reciprocal maps in (Fig. 10(a)] is pseudomorphically strained with no signature of relaxation. The diffraction feature corresponding to the InGaAs QW layer lies exactly underneath the substrate (GaAs) feature with several Pendellösung fringes seen along the vertical direction (Q_z). It confirms that the sample A is of

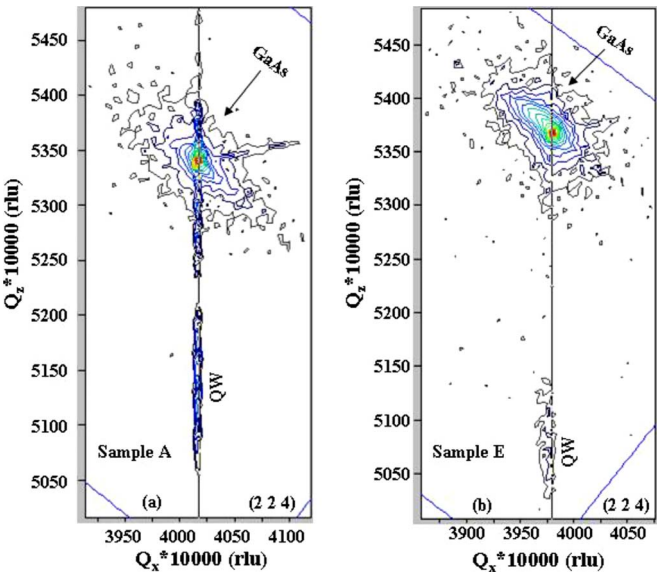

FIG. 10. (Color online) HRXRD reciprocal space maps for the two samples, (a) Sample A, (b) Sample E. QW feature for sample E is clearly shifted in horizontal direction with respect to the substrate feature indicating a possible partial relaxation of the InGaAs QW layer.

very high-crystalline quality without any layer relaxation. We observed almost similar results for samples B, C, and D whereas the situation is a bit different for sample E as shown in Fig. 10(b). Here, the layer feature is slightly shifted in the horizontal direction (Q_x) with respect to the substrate feature indicating some amount of relaxation in the QW. We calculated the parallel (in-plane) and perpendicular (out-of-plane) lattice mismatches normally known as $\varepsilon_{\parallel}$ and $\varepsilon_{\perp}$, respectively, for the sample E and evaluated the relaxation (R%) which is normally defined as the ratio of parallel mismatch to the bulk mismatch for epitaxial layers. The relaxation for sample E is about 3.4% with the mismatch values of $\varepsilon_{\parallel} \sim 0.099\%$ and $\varepsilon_{\perp} \sim 5.35\%$, respectively. We then tried to incorporate the measured value of relaxation in our HRXRD simulations and found that the indium-content for sample E increases only by 1% which in fact lies within the error bar shown in Table I. A careful observation reveals that there is a little relaxation seen even for sample D ($R \sim 1.3\%$). This however does not make any observable difference to the QW parameters measured from the HRXRD simulations. Hence, it is confirmed that the issue of partial relaxation, which is though very important for highly strained epitaxial layers, seems largely insignificant for the present set of InGaAs/GaAs QW samples. It does not affect the measured value of the bowing parameter including its functional dependence in our samples. Finally, we should comment on the large elongation of GaAs feature for sample E in Fig. 10(b) when compared with the sample A. A similar observation have been made earlier by Giannini *et al.*[25] where they observed an elongation of QW features for (004) reflection and correlated it with the interface roughening and mosaicity. We understand that the reason for the enhanced elongation of the GaAs feature in sample E is mainly related to the partial relaxation of the QW, which induces a tensile strain in the cap GaAs layer in addition to the interface roughening and mosaicity.

IV. CONCLUSION

Highly strained InGaAs QWs are studied using complementary spectroscopic techniques. PR spectroscopy is found to be the best technique here providing sharp and well defined QW features in addition to the GaAs barrier layer signature. The sharp QW features are then identified by numerically solving the Schrödinger equation for a finite square potential well using the envelope function approximation. The effect of strain in modifying the band structure was also taken into account, including the effect of spin-orbit coupling on the light-hole energy. We were able to identify all the QW features but the indium content required to get a reasonable match was found to be much larger than the value obtained from HRXRD measurements. The systematic HRXRD simulations clearly indicated the absence of any such large error in the QW composition. It thereafter lead to the discovery of the compositional dependence of the bowing parameter for highly strained InGaAs/GaAs QWs where we could identify all the QW transitions by using the QW parameters obtained from HRXRD measurements. It is found that the disorder term "C_e" of the bowing parameters becomes very important in case of highly strained InGaAs QWs, which make the bowing parameter concentration dependent. It is also found here that the band offset is independent of the composition of InGaAs QWs. We do not observe any signature of indium segregation in these QW structures either in spectroscopic or HRXRD characterization because of the low-temperature MOVPE growth. The effect of indium segregation in our samples lies within the error bars defined in HRXRD experiments. Finally, it is also confirmed that the issue of partial relaxation, thought very important for highly strained epitaxial layers, seems largely insignificant for the present set of InGaAs/GaAs QW samples. It does not affect the measured value of the bowing parameter for our samples.

ACKNOWLEDGMENTS

T.K.S. acknowledges B. M. Arora, K. L. Narasimhan, K. C. Rustagi, S. Ghosh, S. D. Singh and other colleagues at SLS for many fruitful discussions.

*Corresponding author. Present address: Dept. of Electrical and Computer Engineering, Carnegie Mellon University, 5000 Forbes Avenue, Pittsburgh, PA 15213, USA. FAX: +91-731-248-8300; tarun@rrcat.gov.in; tksharma@cmu.edu

†Present address: JENOPTIK Diode Lab GmbH, Max-Planck-Straße 2, 12489 Berlin, Germany.

[1] IEEE standard 802.3ae, 2002.

[2] E. Pougeoise, Ph. Gilet, Ph. Grosse, S. Poncet, A. Chelnokov, J.-M. Gerard, G. Bourgeois, R. Stevens, R. Hamelin, M. Hammar, J. Berggren, and P. Sundgren, Electron. Lett. **42**, 584 (2006).

[3] T. K. Sharma, M. Zorn, U. Zeimer, H. Kiessel, F. Bugge, and M. Weyers, IEEE Photon. Technol. Lett. **14**, 887 (2002), and references therein.

[4] I. L. Chen, W. C. Hsu, T. D. Lee, H. C. Kuo, K. H. Su, C. H. Chiou, J. M. Wang, and Y. H. Chang, Jpn. J. Appl. Phys. **45**, L54 (2006).

[5] W. C. Chen, Y. K. Su, R. W. Chuang, H. C. Yu, M. C. Tsai, K. Y. Cheng, J. B. Horng, C. Hu, and S. Tsau, IEEE Photon. Technol. Lett. **20**, 264 (2008).

[6] Y. K. Su, W. C. Chen, C. T. Wan, H. C. Yu, R. W. Chuang, M. C. Tsai, K. Y. Cheng, C. Hu, and S. Tsau, J. Cryst. Growth **310**, 3615 (2008).

[7] A. Mereuta, V. Iakovlev, A. Caliman, L. Mutter, A. Sirbu, and E. Kapon, J. Cryst. Growth **310**, 5178 (2008).

[8] I. L. Chen, W. C. Hsu, T. D. Lee, and C. H. Chiou, Thin Solid Films **515**, 4522 (2007).

[9] F. Bugge, U. Zeimer, R. Staske, B. Sumpf, G. Erbert, and M. Weyers, J. Cryst. Growth **298**, 652 (2007).

[10] T. K. Sharma, M. Zorn, U. Zeimer, H. Kissel, F. Bugge, and M. Weyers, Cryst. Res. Technol. **40**, 877 (2005).

[11] T. K. Sharma, B. M. Arora, S. Kumar, and M. R. Gokhale, J.

Appl. Phys. **91**, 5875 (2002).
[12] T. K. Sharma, S. D. Singh, S. Porwal, and A. K. Nath, J. Cryst. Growth **298**, 527 (2007).
[13] S. D. Singh, S. Porwal, T. K. Sharma, and K. C. Rustagi, J. Appl. Phys. **99**, 063517 (2006).
[14] M. J. Joyce, Z. Y. Xu, and M. Gal, Phys. Rev. B **44**, 3144 (1991).
[15] Z. Hang, D. Yan, F. H. Pollak, G. D. Pettit, and J. M. Woodall, Phys. Rev. B **44**, 10546 (1991).
[16] T. J. C. Hosea, D. Lancefield, and N. S. Garawal, J. Appl. Phys. **79**, 4338 (1996).
[17] W. S. Chi and Y. S. Huang, Semicond. Sci. Technol. **10**, 127 (1995).
[18] T. K. Sharma, T. J. C. Hosea, S. J. Sweeney, and X. Tang, J. Appl. Phys. **104**, 083109 (2008).
[19] K. Muraki, S. Fukatsu, Y. Shiraki, and R. Ito, Appl. Phys. Lett. **61**, 557 (1992).
[20] I. Vurgaftman, J. R. Meyer, and L. R. Ram-Mohan, J. Appl. Phys. **89**, 5815 (2001).
[21] P. F. Fewster and C. J. Curling, J. Appl. Phys. **62**, 4154 (1987).
[22] P. F. Fewster and N. L. Andrew, J. Appl. Phys. **74**, 3121 (1993).
[23] P. F. Fewster, and N. L. Andrew, J. Phys. D: Appl. Phys. **28**, A97 (1995).
[24] T. Fujii and S. Yamazaki, J. Cryst. Growth **146**, 489 (1995).
[25] C. Giannini, M. F. De Riccardis, A. Passaseo, L. Tapfer, and T. Peluso, Appl. Surf. Sci. **115**, 211 (1997).
[26] J. F. Chen, P. Y. Wang, J. S. Wang, N. C. Chen, X. J. Guo, and Y. F. Chen, J. Appl. Phys. **87**, 1251 (2000).
[27] Y. Zou, P. Grodzinski, E. P. Menu, W. G. Jeong, P. D. Dapkus, J. J. Alwan, and J. J. Coleman, Appl. Phys. Lett. **58**, 601 (1991).
[28] G. D. Gilland, Mater. Sci. Eng., R. **18**, 99 (1997).
[29] O. J. Glembocki and B. V. Shanabrook, in *Semiconductors and Semimetals*, edited by D. G. Seiler and C. G. Littler (Academic, San Diego, CA, 1992), Vol. 36, p. 239.
[30] T. J. C. Hosea, Thin Solid Films **450**, 3 (2004).
[31] L. Kronik and Y. Shapira, Surf. Sci. Rep. **37**, 1 (1999). For bandgap determination, see p. 89.
[32] Y. S. Huang and F. H. Pollak, Phys. Status Solidi A **202**, 1193 (2005).
[33] T. K. Sharma, S. Porwal, R. Kumar, and S. Kumar, Rev. Sci. Instrum. **73**, 1835 (2002).
[34] D. E. Aspnes, in *Handbook on Semiconductors*, edited by T. S. Moss (North Holland, New York, 1980), Vol. 2, p. 109 (and references therein).
[35] Y. S. Huang, H. Qiang, F. H. Pollak, G. D. Pettit, P. D. Kirchner, J. M. Woodall, Hans Stragier, and L. B. Sorensen, J. Appl. Phys. **70**, 7537 (1991).
[36] I. H. Tan, G. L. Snider, L. D. Chang, and E. L. Hu, J. Appl. Phys. **68**, 4071 (1990).
[37] S. L. Chuang, *Physics of Optoelectronic Devices* (Wiley-Interscience, New York, 1995).
[38] F. H. Pollak, in *Semiconductor and Semimetal*, edited by T. P. Pearsall (Academic Press, San Diego, CA, 1990), Vol. 32.
[39] J. Arias, I. Esquivias, E. C. Larkins, S. Burkner, S. Weisser, and J. Rosenzweig, Appl. Phys. Lett. **77**, 776 (2000).
[40] S. Subramanian, B. M. Arora, A. K. Srivastava, G. Fernandes, and S. Banerjee, J. Appl. Phys. **74**, 7618 (1993).
[41] L. Lu, J. Wang, Y. Wang, W. Ge, G. Yang, and Z. Wang, J. Appl. Phys. **83**, 2093 (1998).
[42] V. I. Zubkov, M. A. Melnik, A. V. Solomonov, E. O. Tsvelev, F. Bugge, M. Weyers, and G. Tränkle, Phys. Rev. B **70**, 075312 (2004).
[43] X. Letartre, D. Stievenard, and E. Barbier, Appl. Phys. Lett. **58**, 1047 (1991).
[44] D. J. Arent, K. Deneffe, C. V. Hoof, J. D. Boeck, and G. Borghs, J. Appl. Phys. **66**, 1739 (1989).
[45] G. Ji, D. Huang, U. K. Reddy, T. S. Henderson, R. Houdre, and H. Morkoc, J. Appl. Phys. **62**, 3366 (1987).
[46] M. Kudo and T. Mishima, J. Appl. Phys. **78**, 1685 (1995).
[47] K. Radhakrishnan, S. F. Yoon, H. M. Li, Z. Y. Han, and D. H. Zhang, J. Appl. Phys. **76**, 246 (1994).
[48] J. Leymarie, P. Disseix, M. Rezki, C. Monier, A. Vasson, and A. M. Vasson, Mater. Sci. Eng., B **44**, 147 (1997).
[49] J. Barnes, J. Nelson, K. W. J. Barnham, J. S. Roberts, M. A. Pate, R. Grey, S. S. Dosanjh, M. Mazzer, and F. Ghiraldo, J. Appl. Phys. **79**, 7775 (1996).
[50] J. Leymarie, C. Monier, A. Vasson, A. M. Vasson, M. Leroux, B. Courboules, N. Grandjean, C. Deparis, and J. Massies, Phys. Rev. B **51**, 13274 (1995).
[51] W. Z. Shen, W. G. Tang, S. C. Shen, S. M. Wang, and T. Andersson, Appl. Phys. Lett. **65**, 2728 (1994).
[52] L. Feng, Z. Yaohui, J. Desheng, and W. Youxiang, Int. J. Infrared Millim. Waves **13**, 340 (1994).
[53] S. Marcinkevicius, G. Ambrazevicius, T. Lideikis, and K. Naudzius, Solid State Commun. **79**, 889 (1991).
[54] J. P. Reithmaier, R. Hoger, H. Riechert, A. Heberle, G. Abstreiter, and G. Weimann, Appl. Phys. Lett. **56**, 536 (1990).
[55] S. Niki, C. L. Lin, W. S. C. Chang, and H. H. Wieder, Appl. Phys. Lett. **55**, 1339 (1989).
[56] F. Bugge, U. Zeimer, M. Sato, M. Weyers, and G. Trankle, J. Cryst. Growth **183**, 511 (1998).
[57] Y. Q. Wei, S. M. Wang, X. D. Wang, Q. X. Zhao, M. Sadeghi, I. Tangring, and A. Larsson, J. Cryst. Growth **278**, 747 (2005).
[58] L. W. Sung and H. H. Lin, Appl. Phys. Lett. **83**, 1107 (2003).
[59] B. K. Ridley, *Quantum Processes in Semiconductors* (Oxford University Press, New York, 1988), p. 42.
[60] H. H. Tan, P. Lever, and C. Jagadish, J. Cryst. Growth **274**, 85 (2005).